Journal of Geomatics Vol 10 No. 2 October 2016

Temporal dimensions in rice crop spectral profiles

Christos G. Karydas
Mesimeri, P.O. Box 413, 57500 Epanomi, Greece
Email: xkarydas@gmail.com

(Received: May 12, 2016; in final form: Sep 26, 2016)

Abstract: Using a full range hand-held spectrometer (350 nm – 2500 nm), this study examined the temporal profile of the spectral signature of rice crop (*Oryza sativa L.*). It also, examined the effects of illumination geometry for hyperspectral measurements in rice paddies. The study area was located in Axios river plain (Greece), one of the most extended and highly productive rice cultivation areas in Mediterranean ecoregions. The spectral data were collected from a set of 24 experimental plots cultivated with indica type rice, each of them under different fertilisation treatment on eleven different dates during 2014 and 2015 seasons; in total 264 spectral measurements were recorded. Reflectance from the rice paddies showed not to be influenced from the distance of the device from the plot at nadir, but only by the viewing angle, the distance off nadir, and the aspect. The variance between different treatments was found to be about 14% on average, with the maximum variance (35%) recorded on the 80th day after sowing. Comparison of signature shapes between plots, growth stages, or diachronically, was based on the 1st-order derivative of the signatures. Plotting the temporal profile of different indices together with a time series of four rice crop biometrics allowed identification of a time interval of 10 days as optimum for spectra recordings. The perspectives of the study can be seen in the establishment of a protocol of hyperspectral data collection in rice paddies using portable spectrometers and assisting in the use of hyperspectral cameras mounted on unmanned aerial vehicles towards precision farming and rice crop monitoring.

Keywords: Hand-held hyperspectral radiometer, SVC, Crop monitoring, LAI, MCARI

1. Introduction

1.1 Rice cultivation

Rice *(Oryza sativa L.)* is the second largest cereal crop (after wheat) and the most consumed major staple food; for over 4.4 billion people, rice is the basis of their diet, while the demand increases 3% annually. According to the United Nation's Food and Agriculture Organisation (FAO), in 2013 rice was cultivated in 125 countries around the globe, covering an area of approximately 165 million hectares, which comprises more than one-third of the planted continental/land area. The total production of paddy rice was approximately 740 million tons, with 90% produced in Asia, 5% in America, 4% in Africa, and only 1% of the global rice is produced in Oceania (>8 mil ha) and in Europe (>6 mil ha). Concerning average yield, the highest rice yield is produced in Oceania (10 tons/ha) followed by Europe (6 tons/ha) and Americas (5.5 tons/ha) (Botta et al., 2015; Ferrero, 2005; Ferrero and Tinarelli, 2008; Tao et al., 2015).

Rice shows an incredible capacity to get adapted to a great variety of soil and climatic conditions: from rain fed areas of annual rainfall 100 mm (Al Hasa Oasis in Saudi Arabia) to 5000 mm (Myanmar's Araka Coast) (Ferrero and Tinarelli, 2008). Over 85% of the rice area is irrigated, because this method increases yields and irrigated rice covers most of the America, Australia, Europe and significant parts of Asia and Africa. Rice varieties that are suitable for irrigated ecosystems are highly responsive to nitrogen (N) supply, resistant to several pets and diseases and with high yield potential. N is essential for rice, and usually it is the most yield-limiting nutrient in irrigated rice production worldwide (Ladha and Reddy, 2003; Samonte et al., 2006). Rice plants require N at tillering stage to promote growth and to increase the number of panicles. N also plays important role in grain filling stage, improving the photosynthetic capacity, and promoting carbohydrate accumulation in culms and leaf sheaths (Mae, 1997).

1.2 Spectroscopy in rice

Spectroscopy is the study of the interaction between matter and electromagnetic radiation, measured as a response of a target object at many spectral channels and various spectral ranges (Crouch and Skoog, 2007). The spectral measurement devices are referred to as spectrometers. The variable measured is the intensity of light, while the independent variable is usually the wavelength of light, or any other unit directly proportional to the photon energy (Butler and Laqua, 1995).

Although spectroscopy started indoor in the laboratories, lately there has been a significant increase in the number of portable spectrometers possessed by remote sensing (or even non-remote sensing) groups and a boost of outdoor activities. Field spectroscopy helps in a better understanding of interaction between electromagnetic radiation and biophysical objects, than those achieved when aerial or satellite sensors are employed. Field hyperspectral data is also required to calibrate satellite or aerial hyperspectral images (Clark et al., 1995).

The role of remote sensing in detecting and explaining crop heterogeneity, in the framework of precision farming, has been discussed widely up until now. Precision farming involves the observation, impact assessment and timely strategic response to fine-scale variation (or crop heterogeneity) in causative components of an agricultural production process. However, adoption of precision farming could possibly be limited by coarse spatial or spectral resolution, low frequency of coverage, and delays in imaging product delivery when satellite imagery is the main source of information (Jackson, 1984; Zarco-Tejada et al., 2005). A timely and adequate solution in crop and soil diagnosis can alternatively be provided by aerial hyperspectral imagers (Whiting et al., 2006), or by in-situ hyperspectral measurements (Gnyp et al., 2014).

In this direction, Inoue et al. (2012) designed an experiment of combined use of hyperspectral imagery and field hyper-spectrometers in China and Japan with a view to timely predict canopy nitrogen content (CNC) for growth prediction and precision farming applications. They tested several hyperspectral indices with ground plant measurements, concluding that the ratio spectral index (RSI, corresponding to 740 nm and 522 nm) was the most accurate and robust measure for CNC prediction (r^2>0.9).

In an indirect approach for assessing nitrogen requirements for rice crop (Li et al., 2015), spectra measured in soil samples collected from all over China were linked to nitrogen fertilizer rates through the use of the N-prediction model introduced by Stanford (1973) and adopted by the Ministry of Agriculture of China (2014). In this way, aerial imaging is avoided, though soil sampling may be proved even more costly or laborious.

Nitrogen (N) deficiency can be assessed also through leaf radiation, provided that Chlorophyll is an indirect indicator of nitrogen status, thus allowing for rapid N management and monitoring in a precision farming framework (Lee and Searcy, 2000; Jones et al. 2004; Alchanatis et al. 2005; Kim and Reid 2006; Min et al. 2008). In their hyperspectral experimentation in rice cultivation, Wang et al. (2007) indicated that wavelengths in ranges (1100–1150 nm), (700–750 nm), and (550–600 nm) were those where leaf area index (LAI), wet biomass, and dry biomass could be discriminated effectively. Finally, in their attempt to determine principal wavebands and spectral patterns related to nutrient stress, Noh et al. (2004) and Tumbo et al. (2002) have indicated high spectral resolution and accounting for temporal changes as distinct advantages.

1.3 Study objectives

The main aim of this study was to detect and explain the spectral changes in rice crop over an entire cultivation season. The study focused on indica type rice cultivated under Mediterranean conditions. It also aimed to examine the influence of illumination geometry to rice spectral signature and assess signature's deviation from the generic form, across the spectrum, at different growth stages, and for different treatments.

In contrast to tropical and sub-tropical regions around the world, which experience many cultivation seasons within a year, in Mediterranean ecoregions, rice has only one cultivation season per year, approximately from May to October. In European Union, rice cultivation is extended to 430,479 ha (FAOSTAT, 2013) mostly allocated in Po valley in Italy, Guadalquivir valley, Ebro delta, and Valencia in Spain, Tejo and Mondego valleys in Portugal, Thessaloniki and Serres plain in Greece and Rhone delta in France (Ferrero and Tinarelli, 2008).

The specific objectives of the study can be summarised as follows:

1. To check at what degree illumination geometry, e.g. different distance, viewing angle (i.e. nadir vs. off-nadir), or aspect of the spectrometer, could affect reflectance values recorded in rice paddies.
2. To establish a temporal profile of the spectral signature of rice crop under Mediterranean cultivation conditions (the focus is on indica type).
3. To assess what is the optimum time interval of spectral recordings in order to capture rice phenology changes timely.

2. Materials and methods

2.1 Study area

The main rice production zone of Greece is located in Thessaloniki plain, covering a total of 22,400 ha of intensive cultivation (source: Greek Ministry of Agriculture, 2013). This area produces an average yield of 10 ton/ha, the highest in Greece (official national average yield: 8.9 ton/ha). Local cropping system includes mainly rice as monocrop, while yearly the 25% of the area is rotated with maize, alfalfa, or cotton. The weather conditions are of the typical Mediterranean climate, with temperate summers and suitable for rice cultivation -even for genotypes of indica type. Sowing is carried out during May, while harvesting is carried out during September or October, depended on grain moisture levels (which have to be 19 to 21%). Therefore, the biological cycle of the rice plants can reach the satisfactory level of 130-140 days.

The study was carried out in the plots of the Experimental Station of the Plant Breeding and Genetic Resources Institute of the Cereal Institute of Greece (DEMETER), which is located at the south-east edge of Axios river plain, out of Kalochori village, close to the city of Thessaloniki, Greece (40º27’ N, 23º49’50’’ E, 0 m alt.). Axios plain and Strymon plain are the biggest rice cultivation areas in Greece (Figure 1).

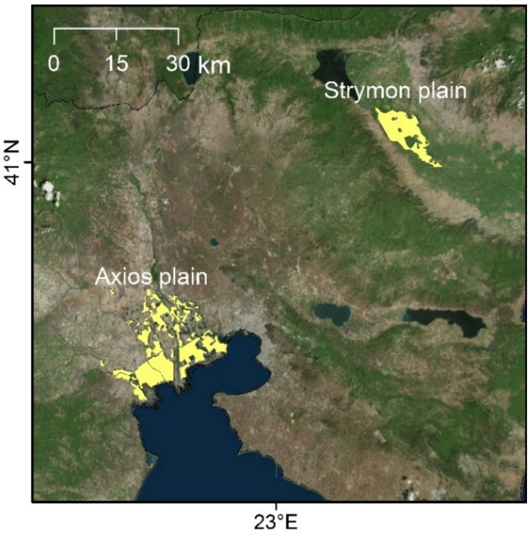

Figure 1: Main rice cultivation sites in Greece (in yellow).

2.2 Plot preparation

Twenty four experimental plots were prepared, covering an area of 11 m^2 each (2.2 m x 5.0 m). The whole process of the preparation of the plots is presented in a video hosted on: http://www.youtube.com/watch?v=3BTt2aF2acs.

Their encoding follows a chess grid system, i.e. A1, A2,…, C8 in a 3x8 arrangement. The soil at the location is silty loam (Aquic Xerofluvents), with a pH of 7.52 and organic matter content of 2.01%.

Seeds of the Greek commercial variety ‘ALEXANDROS’ of indica type were sown on the 20-May-2014 in cement pots with dimensions of 5.00 m x 0.55 m, after 24 hours soaking in water. The paddy-plots were flooded for one day before transplanting. Three hundred sixty (360) seedlings per plot were transplanted by hand into their final positions, when they reached the 3rd to 4th leaf stage on 25-June-2014. Every plot consisted of 15 rows and 24 plants per row, with distances of 20 cm between the rows and 15 cm along the rows. Similar design was followed in 2015, though this time transplanting was conducted about 15 days earlier (Figure 2).

Figure 2: The experimental plots of the Cereal Institute of Greece in Axios plain.

2.3 Hyperspectral measurements

During the 2014 cultivation season, the radiometric measurements were taken at 8 distinct dates from 24 experimental plots (i.e. 192 recordings). Recordings were made only in sunny days from 11:00 to 14:00 o’clock local time. In all cases, the local temperature was below 40º C, as is dictated by the instrument specifications for undisturbed measurements.

The target of each measurement was selected exactly at the middle of the north side of the plot, which practically means that the same plants were captured in every field visit. The recordings were made at a 70-cm distance from the plot at nadir. According to the standard FOV of the device (i.e. FOV=4º) and the specific distance, a circle of about 4.8 cm radius, thus a surface of about 18.7 cm^2, was resulted with every shot (Figure 3). The device was held with a south aspect, i.e. the upper side of the device had a south-looking direction. The specific arrangement will be called from now on ‘standard’.

Reference measurements were taken using Spectralon, approximately every half an hour. Spectralon is the brand name and registered trademark of Labsphere Inc. of a fluoropolymer having the highest diffuse reflectance (Lambertian behaviour) of any known material or coating, over the ultraviolet, visible, and near-infrared regions of the spectrum (Voss and Zhang, 2006).

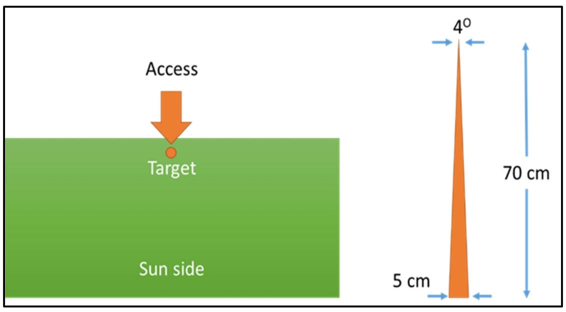

Figure 3: Experimental design of the hyperspectral measurements.

The first measurement of 2014-season was taken on 2-July-2014 and the last on 21-October-2014, i.e. within a total of 111 days, thus covering all critical stages of rice crop growth. The average interval between recordings was about 16 days, the minimum interval was 8 days and the maximum interval was 21 days. After every field visit, the recordings were downloaded from the device and were depicted graphically using the SVC software, thus ensuring their validity and correctness (Figure 4).

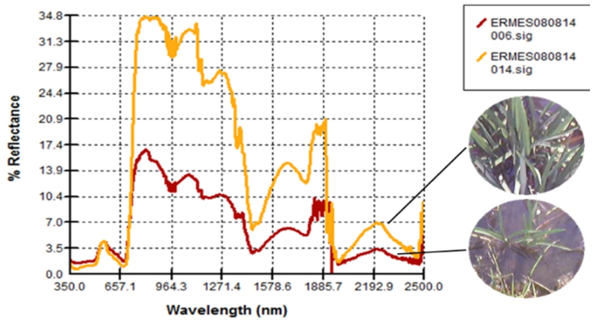

Figure 4: Indicative graphs of reflectance measurements from two different plots.

During the 2015 cultivation season, the spectral measurements were taken on 3 distinct dates from 8 experimental plots; the first recording was conducted on 24-June-2015, the second on 9-July-2015, and the third on 30-July-2015. Again, measurements were taken only in sunny days from 11:00 to 14:00 o'clock local time and always with temperatures below 40^o C. Reference measurements were taken with Spectralon.

On 24-June-2015, measurements were taken from 8 plots at nadir under differentiated distances of the spectrometer from the target; two distances were tested: 70 cm and 10 cm, thus resulting in 16 recordings (1 date x 8 plots x 2 distances). On the same date, another 16 off-nadir measurements were taken from the same plots, this time at 10 cm and at 2 m, thus resulting in 16 recordings (1 date x 8 plots x 2 distances) (Figure 5).

As it is known, with the same FOV, captured surfaces change with distance; for 10 cm distance, the diameter of the surface is 0.7 cm and the extent 0.4 cm^2, for 70 cm the diameter of the surface is 4.8 cm and the extent is 18.7 cm^2, whereas at 2 meters distance, the diameter of the surface is 14 cm and the extent is 150 cm^2.

In the first case, the captured surface becomes extremely small, thus increasing substantially the uncertainty of the spectral measurement.

On 9-July-2015, four measurements were taken from each plot at nadir at a 70-cm distance, while differentiating aspect of the upper side of the device, i.e. south-looking, west-looking, north-looking, and east-looking; as a result, 32 recordings were taken (1 date x 8 plots x 4 aspects). Certainly, the shots did not capture the same plant, but can be considered equivalent, because each plot was under a specific treatment and the distance between the measurements was less than 5 meters in all cases.

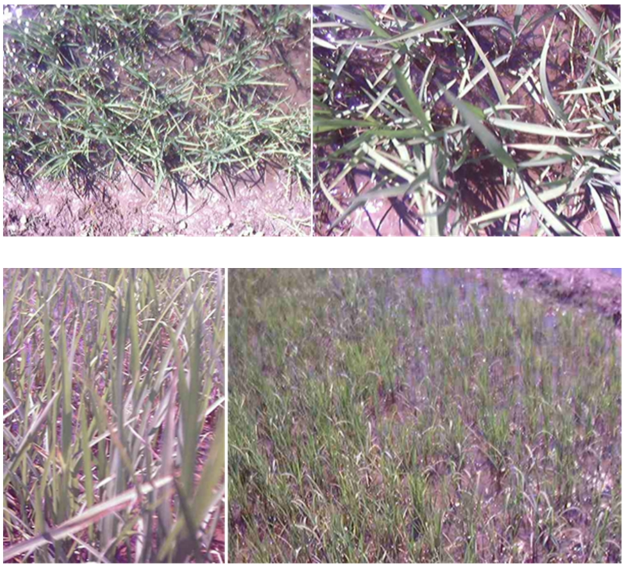

Figure 5: Indicative shots taken at nadir (up) at 70 cm (left) and 10 (right) cm distance and off-nadir (bottom) at 10 cm (left) and 2 m (right) distance, respectively.

Measurements taken on 30-July-2015 from the same plots as the other dates (8 recordings) –together with the other dates- were used to verify the temporal profiles of the signature derived from 2014 data.

In summary, 72 recordings were taken in 2015 and 264 recordings from both years.

3. Results and discussion

3.1 Effects of illumination geometry

From the measurements taken on 24-June-2015 at nadir at 70 cm and 10 cm and off-nadir at 10 cm and at 2 m, four different averaged spectral signatures were derived, one for each of the differentiated illumination geometries (Figure 6). As it can be seen from the shape of the signature curves, the averaged signatures at nadir do not differ substantially between them throughout the entire wavelength range. Possible differentiations between plots (thus between different treatments) are due mainly to domination of water over vegetation or the inverse.

From the measurements taken on 9-July-2015, four different averaged spectral signatures were derived, one for each of the aspects (north-looking, west-looking, south-looking, and east-looking) (Figure 7).

As it can be seen from the shape of the signature curves, only the north-looking signature is found quite lower than the other three aspects in most of the wavelengths.

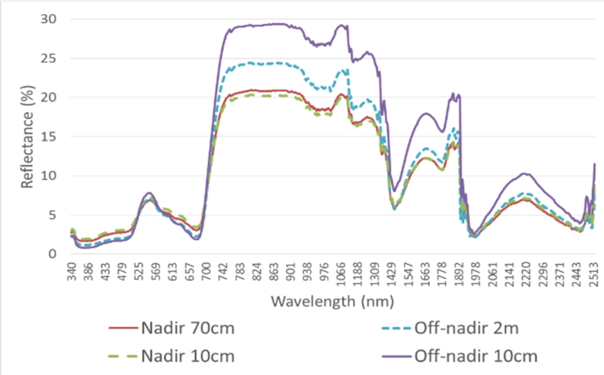

Figure 6: The averaged signatures at nadir and off nadir at different distances derived from 2015 spectral data.

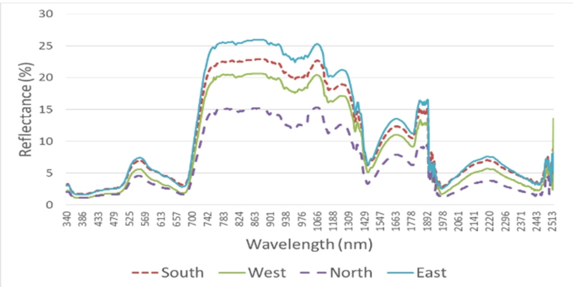

Figure 7: The averaged signatures of the same plots from different aspects derived from 2015 spectral data.

3.2 The spectral signatures

As a result of the spectral recordings at 24 plots over 8 different dates during 2014, 192 original signatures were derived. The shapes of the signature were influenced mostly by the date of recordings rather than the specific plot and therefore signatures were averaged per date. The recording dates were converted into days after sowing in order to be linked easily to a specific growth stage of the rice crop (although this depends on several particularities of the cultivation season, e.g. weather, etc.) (Figure 8).

However, significant variation in spectral signatures was also detected among different plots (and thus treatments) on the same date. These differences were illustrated in terms of maximum difference between the plots (i.e. the maximum spectral value minus the minimum one per wavelength). As a result of averaging all recordings, a typical spectral signature of rice was derived. The average variance reflectance was about 14%, while the maximum recorded variance was 35% detected on the 80th day after sowing (Figure 9).

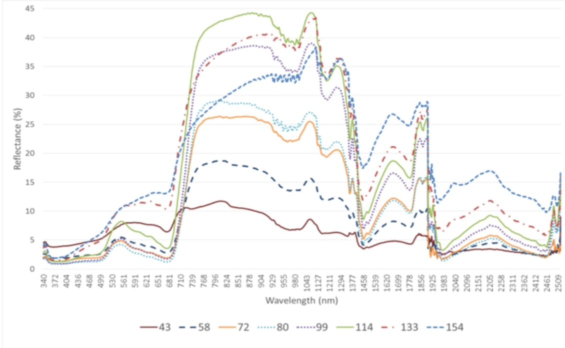

Figure 8: Averaged spectral signature of rice plots at different days after sowing.

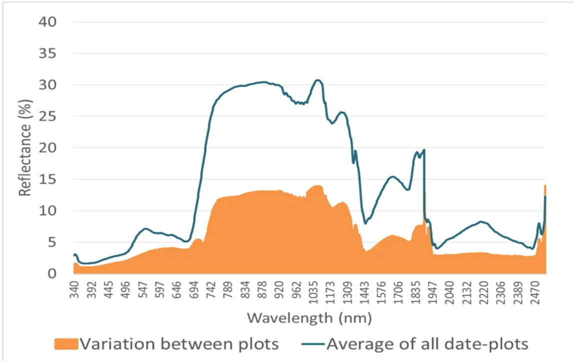

Figure 9: The averaged spectral signature of all recordings in the 2014 season and the recorded variation (as maximum difference) between the rice plots.

Therefore, stage of growth was found to be more determining in rice signature shape rather than the fertilisation treatment.

By comparing visually the signatures of the two examined seasons, the 2014-season was found to be lagging behind that of 2015 quite enough, possibly due to late sowing. The degree of this temporal difference between the two seasons was assessed by matching different signatures from both years, thus indicating a difference of about 16 days; for example, the signature of 25-July-2014 was found to be matching with the signature of 9-July-2015, better than other dates of 2014. But still some differences in the shape of the signature curves –especially in the visible and NIR wavelengths- were detected (Figure 10).

In order to compare the shapes of the two signatures in more detail, the 1st–order derivative of the two reflectance curves were plotted in a common graph, focusing to the spectral wavelengths of interest. Examination of the derivatives of the spectral signature curves was considered to be an appropriate method of comparison between the shapes of the signatures, as derivatives are normalised expressions by default. Liu et al. (2010) have used 1st and 2nd

order derivatives of the reflectance (FDR and SDR, respectively) in order to characterise rice panicles as for their health under laboratory conditions, while Gnyp et al. (2014) used to optimise above ground biomass estimations based on narrow band vegetation indices.

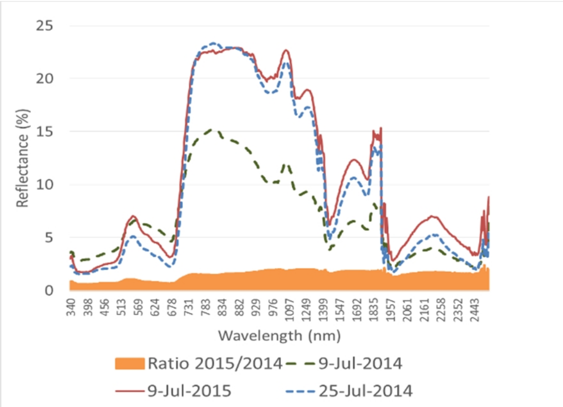

Figure 10: Comparison of rice signatures from the two examined seasons (2014-2015) in a common graph.

Examination of the FDRs of the 25-July-2014 and 9-July-2015 signatures, indicated that significant differences between the two signatures were found in the spectral range 690-850 nm (Figure 11).

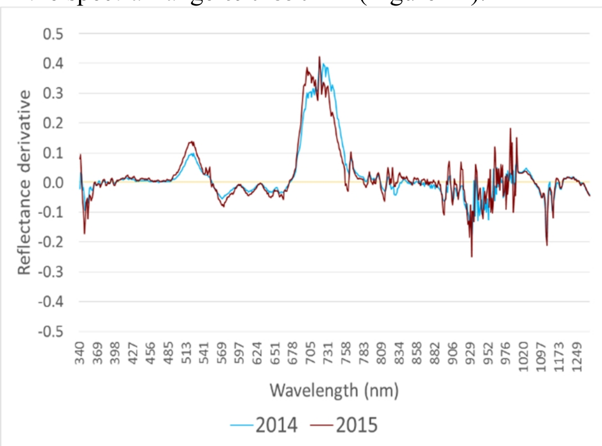

Figure 11: The 1st-order derivative of two equivalent signatures from 2014 and 2015 data collections (25-July-2014 and 9-July-2015) plotted in a common graph (focusing to the spectral wavelengths of interest).

Using the derivatives of signatures three characteristic dates (i.e. 31-Jul-2014, 11-Sep-2014, and 21-Oct-2014), which correspond to 72, 114, and 154 days after sowing, showed that the latter signature differs substantially in shape by the other two, especially in the blue and red wavelengths, as well as in the early NIR region (Figure 12).

Figure 12: The 1st derivative of three characteristic dates (i.e. 31-Jul-2014, 11-Sep-2014, and 21-Oct-2014), which correspond to 72, 114, and 154 days after sowing.

3.3 Optimum time-interval

In order to determine the optimum time-interval between rice crop spectra recordings, a set of measurements of fundamental rice biometrics (i.e. plant height, chlorophyll content index –CCI-, biomass, and Nitrogen content) together with two well-established vegetation indices were plotted across recording dates in a common graph.

It is known that many vegetation indices show better sensitivity than individual spectral bands for the detection of biomass and several other biometrics (Asrar et al., 1984). In this study, the rice crop spectra were used to calculate Leaf Area Index (LAI) estimations based on the Perpendicular Vegetation Index (PVI), according to a methodology developed by Shibayama and Munakata (1986):

$$LAI = 0.022 \cdot PVI^{1.7} \quad (r^2=0.9)$$

where PVI is defined as follows:

$$PVI = 0.778 \cdot R840 - 0.628 \cdot R660 - 1.35$$

where $Rxxx$ the reflectance of rice crop at the *xxx* nm wavelength (here 840 and 660 nm).

It should be noted, however, that these equations were derived under slightly different conditions than those under which the current measurements were taken: with a 15° FOV and 2.5 m distance at nadir, thus resulting in a 60 cm diameter captured surface; also, the bandwidth was defined between 5 and 10 nm depending on the wavelength.

Also, the rice crop spectra were used to calculate the Modified Chlorophyll Absorption Ratio Index (MCARI), which is used broadly as an appropriate index of chlorophyll absorption throughout the cultivation season. According to Daughtry et al.

(2000), MCARI is defined by the following equation:

$$MCARI = [(R700 - R670) - 0.2 \cdot (R700 - 550)] \cdot (\frac{R700}{R670})$$

The LAI and MCARI values derived from the rice crop spectra as per date average of the recordings from the 2014 season, were plotted together vs. days after sowing; thus, revealing characteristic shapes of the growth curves in terms of crop extension (LAI) and vigour (MCARI).

The time step implemented for spectral data collection during the 2014 season was 16 days on average. This interval was not always adequate in order to capture important phenology changes of rice crop, as it can be indicated when several biometrics measured during the 2014 season by the Cereal Institute of Greece, are plotted across dates of hyperspectral measurements (e.g. between 80 and 100 days after sowing) (Figure 13).

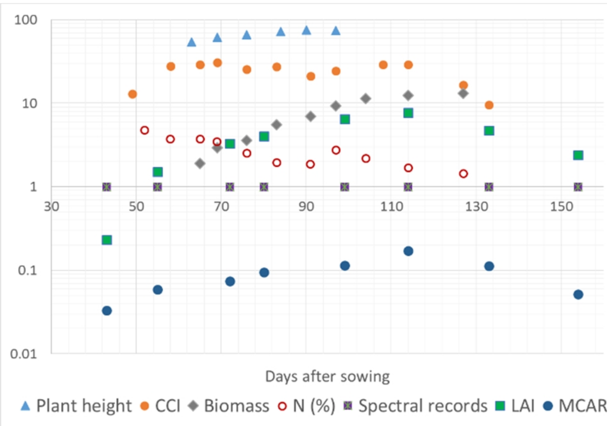

Figure 13: Time series plot of plant height, chlorophyll content index (CCI), biomass, and Nitrogen content, together with spectral-derived LAI and MCARI vs. dates of hyperspectral measurements (y-axis in logarithmic scale).

4. Conclusions and outlook

It is known that rice (*Oryza sativa L.*) paddies are mixtures of the most common biophysical features, i.e. vegetation, water, and soil, in complex spatiotemporal patterns. This study was the first to develop a temporal profile of the spectral signature of rice, based on intensive measurements from multiple dates, years, and treatments of the indica type commercial variety 'Alexandros' under Mediterranean cultivation conditions.

Illumination geometry was found to be critical in spectral recordings of rice paddies. Viewing angle (nadir vs. off nadir), distance of the device from the plot off nadir, and aspect of the device at nadir resulted in big deviations from the 'standard' measurements taken from the same plots at 70 cm distance at nadir. In contrast, distance did not affect measurements a lot when the device was recording at nadir.

The spectral signatures of rice paddies showed to be influenced significantly by the date of recordings rather than the specific treatment; but still, half of the dates had signatures with similar shapes. In order to compare signatures between plots or crop growth stages and diachronically, the derivatives of the reflectance curves were used.

With regard to different treatments at the same date, the reflectance variance was about 14%, with the maximum variance 35% on the 80th day after sowing. However, all treatments (plots) recorded at the same date seem to follow the same curve shape with the exception only of the very early growth stages (especially the 43rd day after sowing).

Deriving the temporal profile of different indices (LAI and MCARI) together with a time series of four rice crop biometrics allowed identification of a time interval of 10 days as optimum step: 5 days were found necessary during the intensive growth periods, while a 15-day step would be enough for slow growth periods. In general, eight measurements distributed accordingly could be suggested for the entire cultivation period.

The experience gained from this study will help in establishing a protocol of hyperspectral data collection from rice fields, using portable hyper-spectrometers, with regard to limitations, assumptions, and practical issues of in situ recordings. It will also help the potential use of hyperspectral cameras mounted on an unmanned aerial vehicle (UAV) for precision farming applications.

Acknowledgments

Many thanks to the Aristotle University of Thessaloniki, Lab of Forest Management and Remote Sensing for the availability of the SVC-1024i spectrometer. Also, the Hellenic Agricultural Organization - DEMETER, Institute of Plant Breeding and Genetic Resources, for the provision of the experimental plots and the biometric values collected from the Kalochori Experimental Station.

Conflicts of Interest

The author declares no conflict of interest.

References

Alchanatis, V., Z. Schmilovitch and M. Meron (2005). In-field assessment of single-leaf nitrogen status by spectral reflectance measurements. *Precision Agric.* 69(1), 25-39.

Asrar, G., M. Fuchs, E.T. Kanemasu and J.L. Hatfield (1984). Estimating absorbed photosynthetic radiation and leaf area index from spectral reflectance in wheat. *Agron. Journal* 76: 300-306.

Botta, G.F, A. Tolón-becerra, X. Lastra-bravo, R. Hidalgo, D. Rivero and D. Agnes (2015). Alternatives for handling rice (Oryza sativa L.) straw to favor its decomposition in direct sowing systems and their incidence on soil compaction. *Geoderma* 2015, 239–240, 213–222.

Butler, L.R.P. and K. Laqua (1995). Nomenclature, symbols, units and their usage in spectrochemical analysis-IX. Instrumentation for the spectral dispersion and isolation of optical radiation (IUPAC Recommendations 1995). *Pure Appl. Chem.* (IUPAC) 67 (10): 1725–1744.

Clark, R.N., T.V.V. King, C. Ager and G.A. Swayze (1995). Initial vegetation species and senescence/stress mapping in the San Luis Calley, Colorado using imaging spectrometer data. Proceedings: Summitville Forum '95, H.H. Posey, J.A. Pendelton, and D. Van Zyl Eds., Colorado Geological Survey Special Publication 38, p. 64-69.

Crouch, S. and D.A. Skoog (2007). Principles of instrumental analysis. Australia: Thomson Brooks/Cole.

Daughtry, C.S.T., C.L. Walthall, M.S. Kim and E. Brown De Colstoun (2000). Estimating corn leaf chlorophyll concentration from leaf and canopy reflectance, *Remote Sens. of Environ.*, 74: 229-239.

Ferrero, A. (2005). Preface. In Rice Landscapes of Life, Ferrero, A., Scansetti, M., Eds., Edizioni Mercurio: Vercelli, Italy, 2005, p. 207.

Ferrero, A. and A. Tinarelli (2008). Rice cultivation in the EU ecological conditions and agronomical practices, In Pesticides Risk Assessment in Rice Paddies: Theory and Practices, 1st ed., Capri, E., Karpouzas, D.G., Eds., Elsevier Science: Amsterdam, The Netherlands, 2008, pp. 1-24.

Gnyp, M.L., Y. Miao, F. Yuan, S.L. Ustin, K. Yu, Y. Yao, S. Huang and G. Bareth (2014). Hyperspectral canopy sensing of paddy rice aboveground biomass at different growth stages. *Field Crops Research*, 155:42-55.

https://archive.org/details/RiceAlmanac. IRRI, Rice Almanac Source book for One of the Most Important Economic Activities on Earth, 4th ed, pp 283. Available online: (last accessed on 20-March-2016).

http://faostat3.fao.org/home/E FAOSTAT, Statistical data: (last accessed on 20-March-2016).

http://www.moa.gov.cn/ztzl/ctpfsf/gzdt/201109/P020110922365288911962.doc. Ministry of Agriculture of the People's Republic of China. Protocols of Soil Testing and Formulated Fertilization Technology. Available online: (last accessed on 20-March-2016).

Inoue, Y., E. Sakaiya, Y. Zhu and W. Takahashi (2012). Diagnostic mapping of canopy nitrogen content in rice based on hyperspectral measurements, *Remote Sens. of Environ.* 2012, 126, 210-221.

Jackson, R.D. (1984). Remote sensing of vegetation characteristics for farm management. SPIE 475:81-96.

Jones, C.L., N.O. Maness, M.L. Stone and R. Jayasekara (2004). Chlorophyll estimation using multi-spectral reflectance and height sensing. Technical presentation made on August 1, 2004 at 2004 ASAE/CSAE Annual International Meeting. ASAE/CSAE Paper No. 043081. ASAE, 2950 Niles Rd., St. Joseph, MI 49085-9659 USA.

Kim, Y., and J.F. Reid (2006). Modeling and calibration of a multi-spectral imaging sensor for in-field crop nitrogen assessment. *Applied Eng. in Agric.* 2006, 22(6), 935-941.

Ladha, J.K. and P.M. Reddy (2003). Nitrogen fixation in rice system: State of knowledge and future prospects. *Plant Soil* 2003, 252, 151–167.

Lee, W.S. and S. Searcy (2000). Multispectral sensor for detecting nitrogen in corn plants. Technical presentation made on July 9-12, 2000 at 2000 ASAE Annual International Meeting. ASAE Paper No. 001010. ASAE, 2950 Niles Rd., St. Joseph, MI 49085-9659 USA.

Li, S., W. Ji, S. Chen, J. Peng, Y. Zhou and Z. Shi (2015). Potential of VIS-NIR-SWIR Spectroscopy from the Chinese Soil Spectral Library for Assessment of Nitrogen Fertilization Rates in the Paddy-Rice Region, China. *Remote Sens.* 2015, 7, 7029-7043.

Liu, Z.Y, J.J. Shi, L.W. Zhang and J.F. Huang (2010). Discrimination of rice panicles by hyperspectral reflectance data based on principal component analysis and support vector classification, *J Zhejiang Univ-Sci B (Biomed & Biotechnol)* 11(1):71-78.

Mae, T. (1997). Physiological nitrogen efficiency in rice: Nitrogen utilization, photosynthesis, and yield potential. *Plant Soil* 1997, 196, 201-210.

Min, M., W.S. Lee, T.F. Burks, J.D. Jordan, A.W. Schumann, J.K. Schueller and H. Xie (2008). Design of a hyperspectral nitrogen sensing system for orange leaves. *Computers and Electronics in Agric.* 2008, 63(2), 215-226.

Noh, H.K., Q. Zhang and S. Han (2004). Sensor-based variable-rate application of nitrogen by using multi-spectral image sensor. Technical presentation made on August 1, 2004 at 2004 ASAE Annual International Meeting. ASAE Paper No. 041133. ASAE, 2950 Niles Rd., St. Joseph, MI 49085-9659 USA.

Samonte, S.O.P.B., L.T. Wilson, J.C. Medley, S.R.M.C. Pinson, A.M.M. Clung and J.S. Lales (2006). Nitrogen utilization efficiency: relationships with grain yield, grain protein, and yield-related traits in rice. *Agro J.* 2006, 98, 168-176.

Shibayama, M. and K. Munakata (1986). A spectroradiometer for field use. III. A comparison of some vegetation indices for predicting luxuriant paddy rice biomass. *Japan. Jour. Crop Sci.* 55(1):47-52.

Stanford, G. (1973). Rationale for optimum nitrogen fertilization in corn production. (1973). *J. Environ. Qual.* 1973, 2, 159–166. 32.

Tao, Y., Y. Zhang, X. Jin, G. Saiz, R. Jing, L. Guo, M. Liu, J. Shi, Q. Zuo, H. Tao, K. Butterbach-Bahl, K., Dittert and S. Lin (2015). More rice with less water - Evaluation of yield and resource use efficiency in ground cover rice production system with transplanting. *European J. Agron.* 2015, 68, 13–21.

Tumbo, S.D., D.G. Wagner and P.H. Heinemann (2002). On-the-go sensing of chlorophyll status in corn. Transactions of the ASAE 2002, 45(4), 1207–1215, doi: 10.13031/2013.9929.

Voss, K.J. and H. Zhang (2006). Bidirectional reflectance of dry and submerged Labsphere Spectralon plaque. *Applied Optics* 45 (30): 7924–7927.

Wang, F.M., J.F. Huang and X.Z. Wang (2007). Identification of Optimal Hyperspectral Bands for Estimation of Rice. *Biophysical Parameters Acta Botanica Sinica* 2007, 50(3), 291—299.

Whiting, M.L., S.L. Ustin, P. Zarco-Tejada, A. Palacios-Orueta and V.C. Vanderbilt (2006). Hyperspectral mapping of crop and soils for precision agriculture. In Proc. SPIE 6298, Remote Sensing and Modeling of Ecosystems for Sustainability III, San Diego, California, USA, August 13, 2006, Wei Gao, Susan L. Ustin, Eds (doi:10.1117/12.681289).

www.youtube.com/watch?v=3BTt2aF2acs (Hellenic Agricultural Organization – Institute of Plant Breeding and Genetic Resources, Kalochori Experimental Station. Preparation of rice experimental plots on YouTube). (last accessed on 20-March-2016).

www.spectravista.com/HR1024i.html. (Spectral Vista Corporation, SVC HR-1024i) (last accessed on 20-March-2016).

Zarco-Tejada, P.J., S.L. Ustin and M. Whiting (2005). Temporal and spatial relationships between within-field yield variability in cotton and high-spatial hyperspectral remote sensing imagery. *Agronomy Journal* 97(3): 641-653.